Electronic Supplementary Material (ESI) for Environmental Science: Nano.

Rational design of a FRET based nanoprobe of gold conjugated carbon dots for simultaneous monitoring and disruption of *Pseudomonas aeruginosa* biofilm through selective detection of virulence factor pyocyanin

Chandni Sharma,[1,2] Ashish K Shukla[1,2] and Amitabha Acharya[1,2*]

[1]*Biotechnology Division, CSIR-Institute of Himalayan Bioresource Technology, Palampur (H.P.) 176061, India*

[2]*Academy of Scientific and Innovative Research (AcSIR), Ghaziabad- 201002, India*

[*]Author to whom the correspondence should be addressed, E-mail: amitabhachem@gmail.com; amitabha@ihbt.res.in; Tel (off): +91-1894-233339; Extn. 397; Fax: +91-1894-230433.

Experimental Section

S01. (a) Materials

Poly(ethylene glycol) bis (3-aminopropyl) terminated (PEG_{1500N}), tetrachloroaurate (III) hydrate, pyocyanin, pyoverdine, glucose, ascorbic acid, fibrinogen, iron (II) chloride tetrahydrate, iron (III) chloride hexahydrate, potassium chloride, lead (II) nitrate, silver nitrate, zinc chloride, rhodamine 101, rhodamine 6G, sodium azide, 2-acetylanthracene, 9-anthracenemethanol, tryptophan, hydrophobic Durapore membrane filter and dialysis tubing cellulose membrane were purchased from Merck Sigma-Aldrich, USA. Tri-sodium citrate, sodium hydroxide, aluminium chloride anhydrous, copper (II) sulphate pentahydrate and cadmium chloride monohydrate were purchased from SDFCL, India. Nutrient agar, nutrient broth, human serum albumin, transferrin, sodium bicarbonate, sodium acetate, sodium bromide, sodium sulphate, calcium chloride anhydrous, magnesium chloride hexahydrate, manganese chloride tetrahydrate, sodium chloride and nickel (II) sulphate hexahydrate were purchased from HiMedia, India. Sodium carbonate anhydrous, sodium phosphate dibasic dihydrate, sodium phosphate monobasic dihydrate and cobalt (II) nitrate were purchased from SRL, India. Gram-positive bacterium *Staphylococcus aureus* (*S. aureus*, MTCC-3196) and Gram-negative bacterium *Pseudomonas aeruginosa* (*P. aeruginosa*, MTCC-741) were procured from Microbial Type Culture Collection and Gene Bank, CSIR-IMTECH, Chandigarh. Syto 9 stain was purchased from Gibco, Invitrogen. Tissue culture coated 6 and 96 well plates were obtained from Eppendorf.

S01.(b) Characterization methods

The morphological studies were performed using Tecnai T20 twin, TEM 200 kV (FEI, Netherlands). For TEM, specimen was prepared by drop casting the sample on carbon-coated copper 300 mesh microgrid followed by drying of all the samples in a desiccator. The particle

size distribution histograms were prepared by using ImageJ software *via* calculating the size of ~ 20-30 NPs by analyzing TEM images. Zeta potential values were measured by taking 1 ml of sample using Zetasizer Nano ZS (Malvern Instruments). The absorption and fluorescence spectra of nanomaterials were analyzed in NanoDrop 2000 UV-Vis spectrophotometer (Thermo Scientific™) and Varian Cary Eclipse fluorescence spectrophotometer (Agilent), respectively. Fluorescence spectroscopy was also done with sample concentration of 1mg/ml. FTIR analysis was performed by using dry samples with IR Affinity-1S Fourier transform infrared spectrophotometer (Shimadzu). Electron spray ionization-mass spectroscopy (ESI-MS) was done using Waters Micromass Q-TOF Ultima Spectrometer. MALDI analysis was done by using UltrafleXtreme, MALDI-TOF/TOF Mass Spectrometer, Bruker corporation. Nuclear magnetic resonance (NMR), X-ray powder diffraction (XRD) and X-Ray Photoemission Spectroscopy (XPS) analysis was done using 600 MHz NMR (AscendTM 600, Bruker), SmartLab 9kW rotating anode X-ray diffractometer (Rigaku Corporation) and Prevac, respectively. For NMR 30 mg of sample was dissolved in DMSO-d_6, whereas XPS and XRD was done with 30 mg of dried samples. Confocal studies were done using Carl Zeiss LSM 510 META. Bacterial, biofilm growth inhibition measurements were done by using Synergy Microplate Reader, Biotek.

S01.(c) Concentration of Au in Au_{Cit}NPs and Au@$OPCD_{PEG}$

Molecular weight of gold salt, [$HAuCl_4$]	=	339.79 g/mol	
Molecular weight of gold	=	196.96 g/mol	
Weight of gold salt taken	=	7.9 mg	
Weight of gold taken	=	(197/339.79)×7.9	=4.58 mg
Volume of gold taken (V)	=	4.58/19.32	=0.000237 cm^3
Average diameter of gold nanoparticles	=	9 nm (r = 4.5 nm)	

Volume of a single gold nanoparticle, (v) = $4/3\pi r^3$ = $4/3\times3.14(4.5\times10^{-9})^3$

= $3.817x10^{-19}$ cm^3

No. of nanoparticles in colloidal solution (N) = V/v $=0.000237/3.81\times10^{-19}$

$=6.22\times10^{14}$ particles

Concentration of nanoparticles =N/final volume of colloidal solution.

$=6.22\times10^{14}/35=1.78\times10^{13}$ particles/ml

$=1.78\times10^{16}$ particles/liter

Concentration of Au in Au_{Cit}NPs in moles $=1.78\times10^{16}/6.023\times10^{23}=2.96\times10^{-8}$ moles

=29.6 nM

10 ml of Au_{Cit}NP used in synthesis of Au@$OPCD_{PEG}$ solution contains=29.6 nM

1 ml of Au_{Cit}NP used in synthesis of Au@$OPCD_{PEG}$ solution contains=29.6/15×10 =19.6 nM

According to volume ratios used in synthesis procedure of Au@$OPCD_{PEG,}$ the Au concentration was found to be 19.6 Nm

Figure S01. Photographic image of nanocomposite

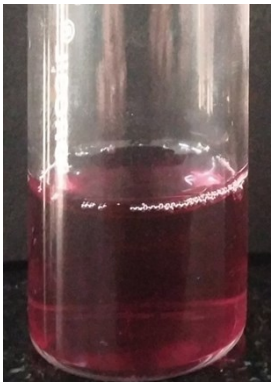

Figure S01. Photographic image of synthesized Au@OPCD$_{PEG}$

Figure S02.TEM, DLS and EDAX studies

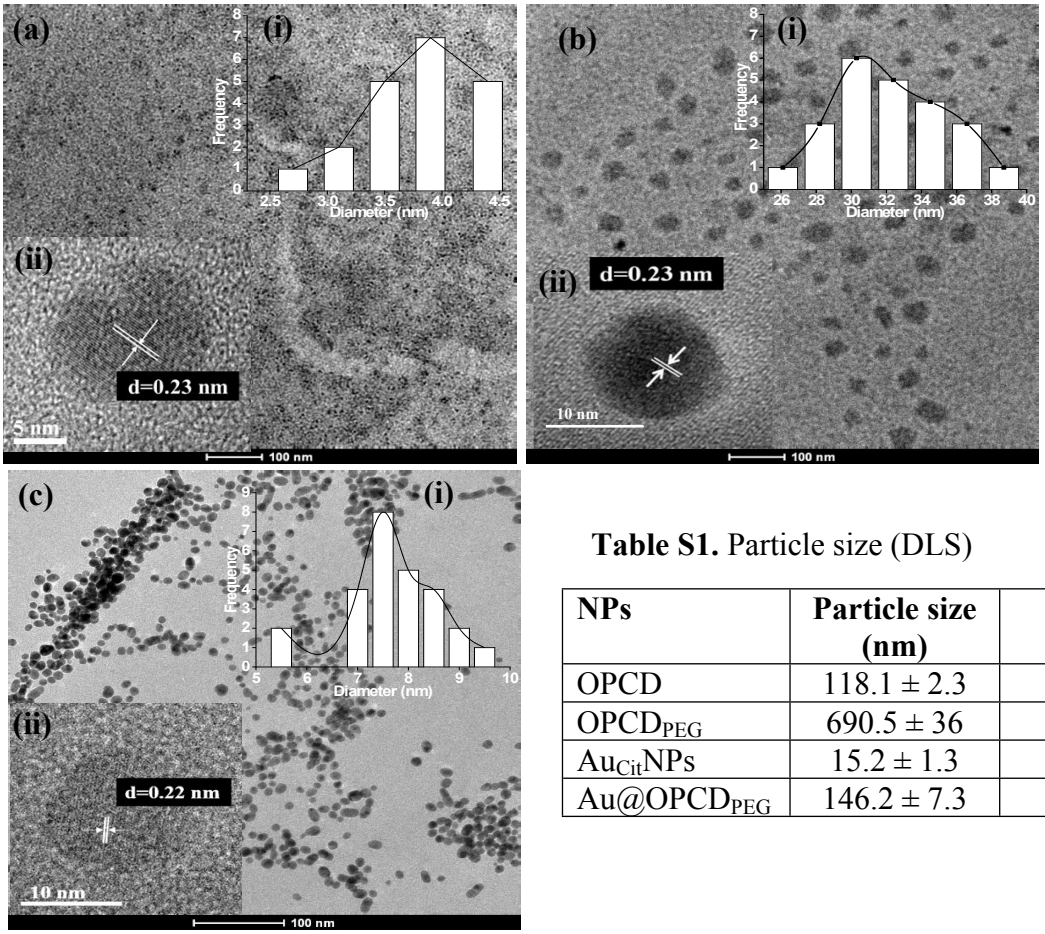

Table S1. Particle size (DLS)

NPs	Particle size (nm)	PDI
OPCD	118.1 ± 2.3	0.24
$OPCD_{PEG}$	690.5 ± 36	0.32
$Au_{Cit}NPs$	15.2 ± 1.3	0.22
$Au@OPCD_{PEG}$	146.2 ± 7.3	0.23

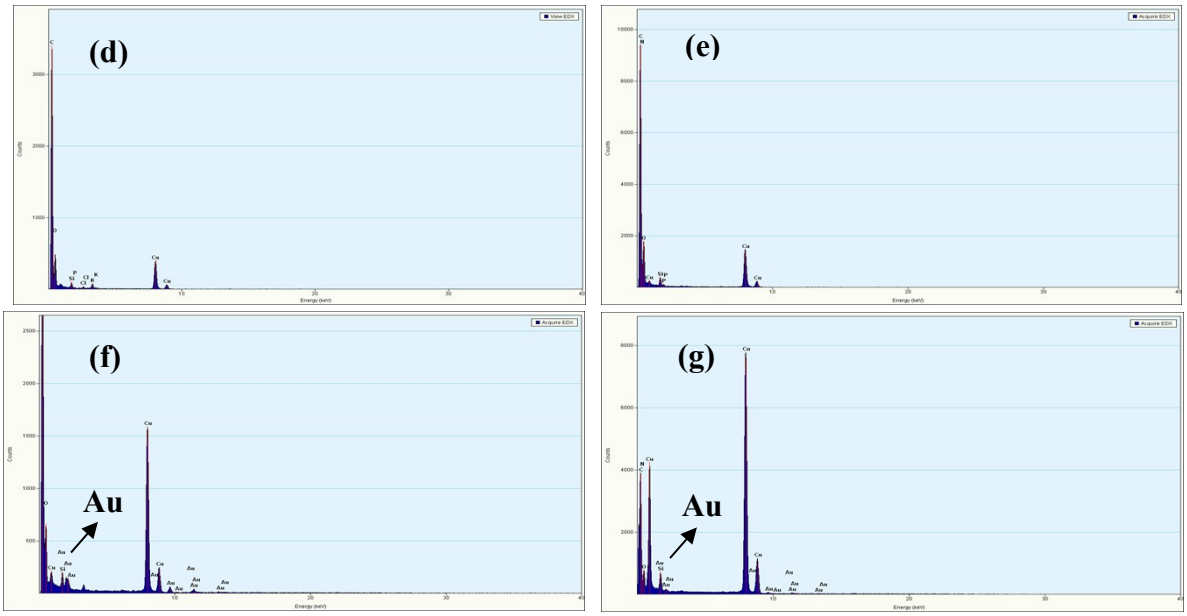

Figure S02. (a) TEM micrographs of OPCD, (b) $OPCD_{PEG}$, and (c) $Au_{Cit}NP$. Average particle size analysis graph and high magnification, TEM images were given in inset for respective NPs i.e, (a-i, ii) OPCD, (b-i, ii), $OPCD_{PEG}$ and (c-i, ii) $Au_{Cit}NPs$. Z-average hydrodynamic size of prepared NPs given in Table S1. (d) Represents EDAX of OPCD, (e) $OPCD_{PEG}$ (f), $Au_{Cit}NP$ and (g) $Au@OPCD_{PEG}$.

Figure S03. Powder-XRD (P-XRD) and SAED studies

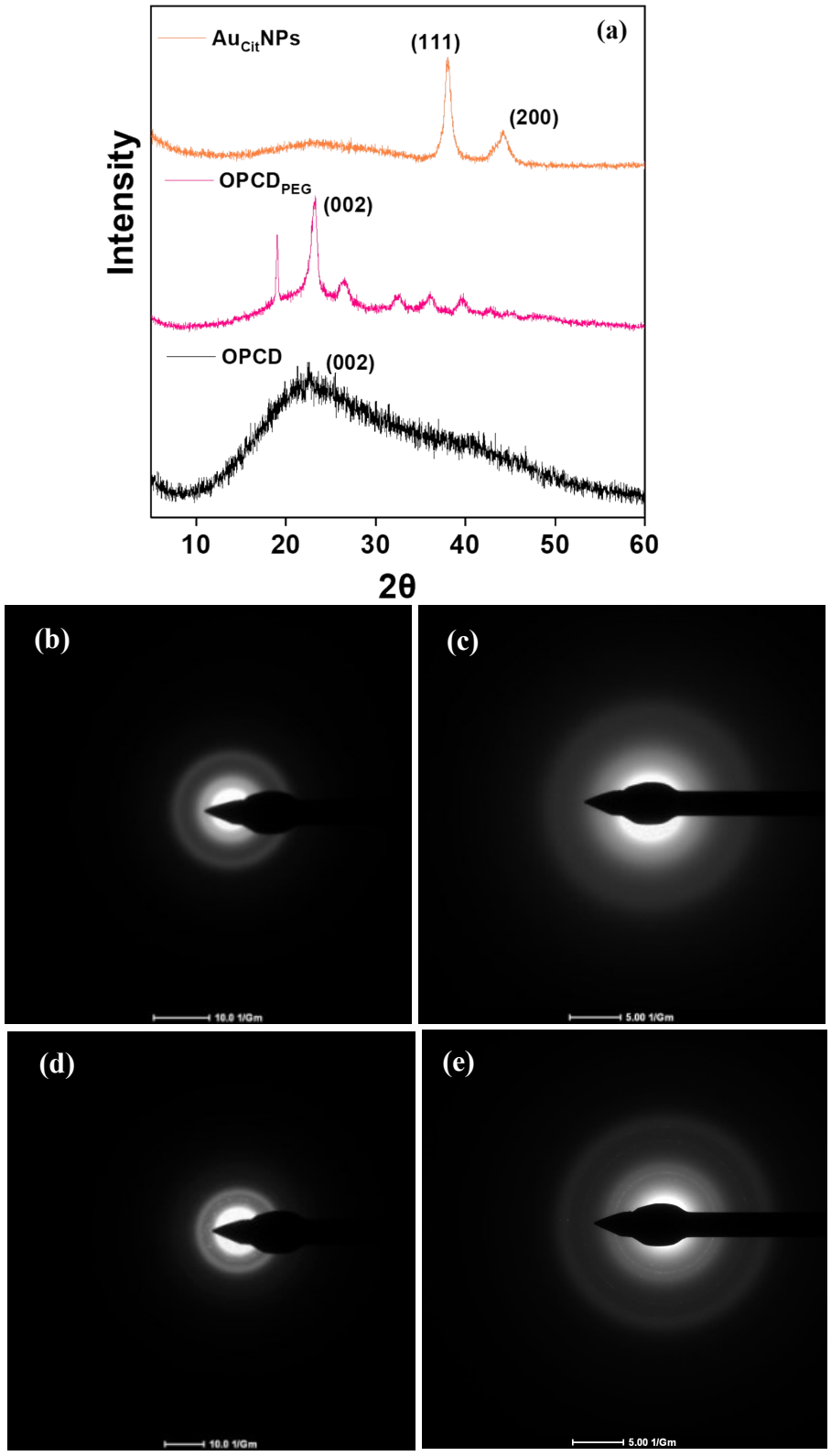

Figure S03. (a) P-XRD and SAED spectra of the synthesized NPs (b) OPCD, (c) $OPCD_{PEG}$ (d) $Au_{Cit}NPs$ and (e) $Au@OPCD_{PEG}$.

Figure S04. XPS spectra

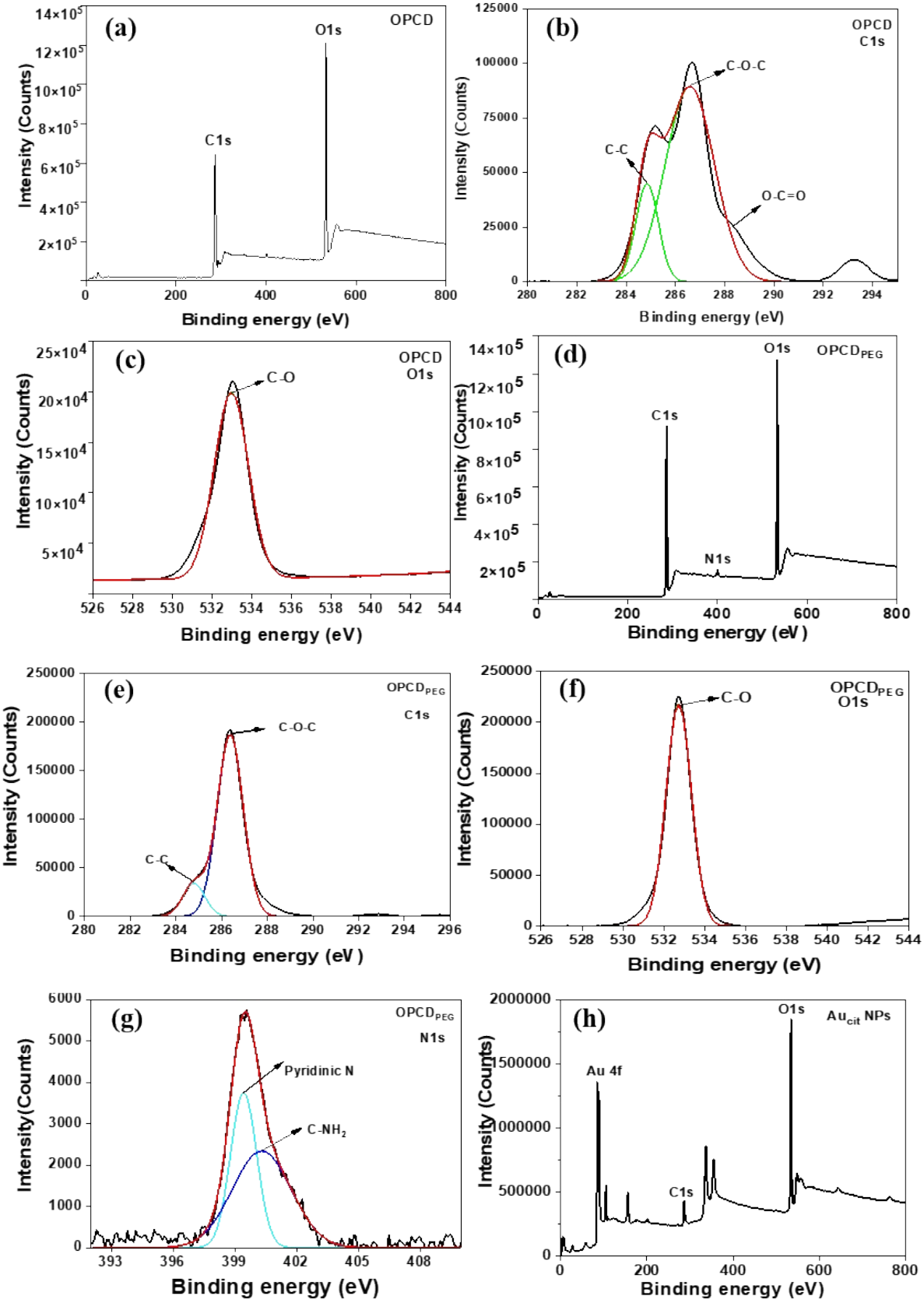

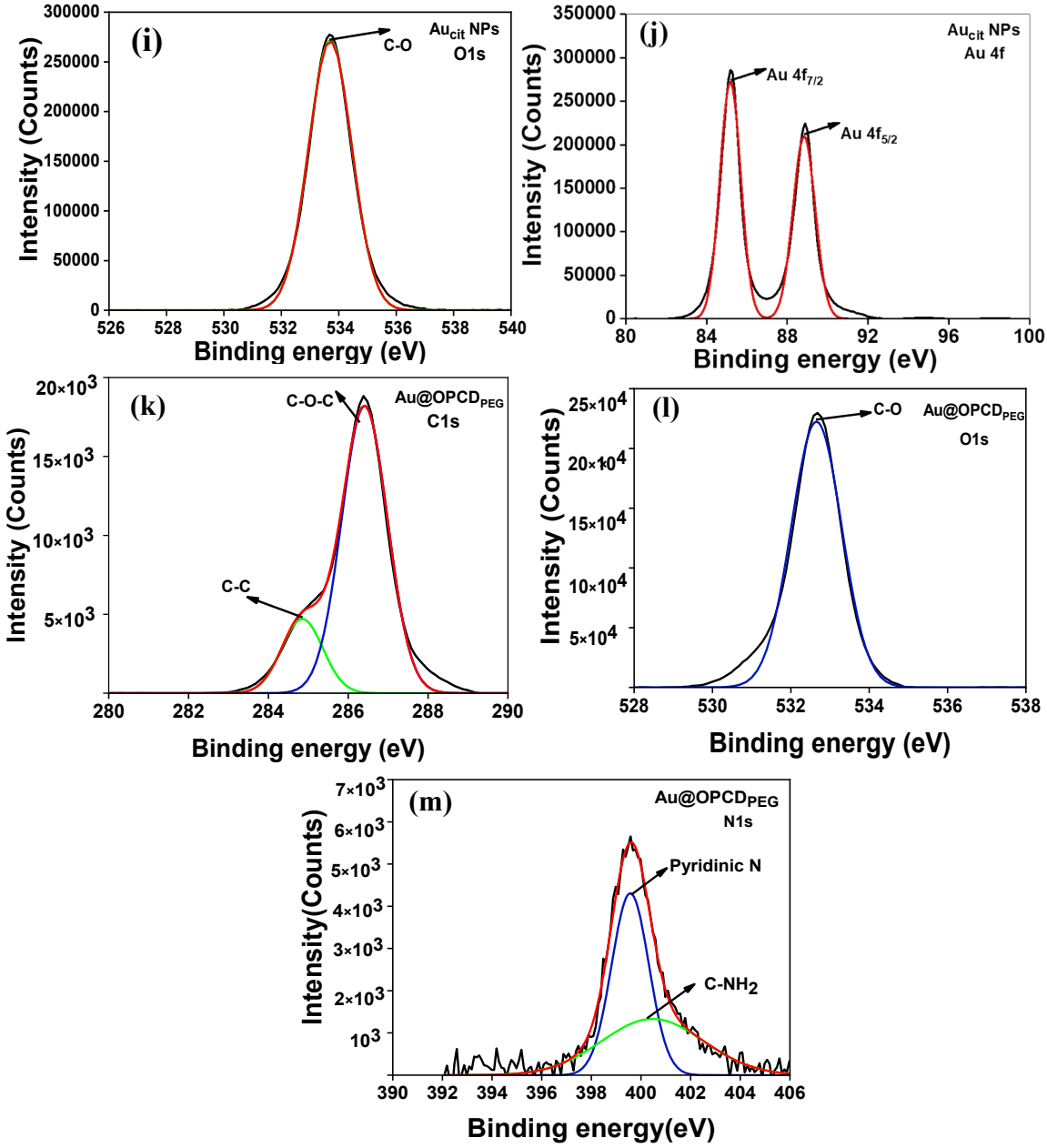

Figure S04. XPS overall and corresponding constituent elemental spectra of synthesized NPs viz., (a-c) OPCD, (d-g) $OPCD_{PEG}$, (h-j), Au_{Cit}NPs and $Au@OPCD_{PEG}$ (k-m).

Figure S05. MALDI and FTIR study

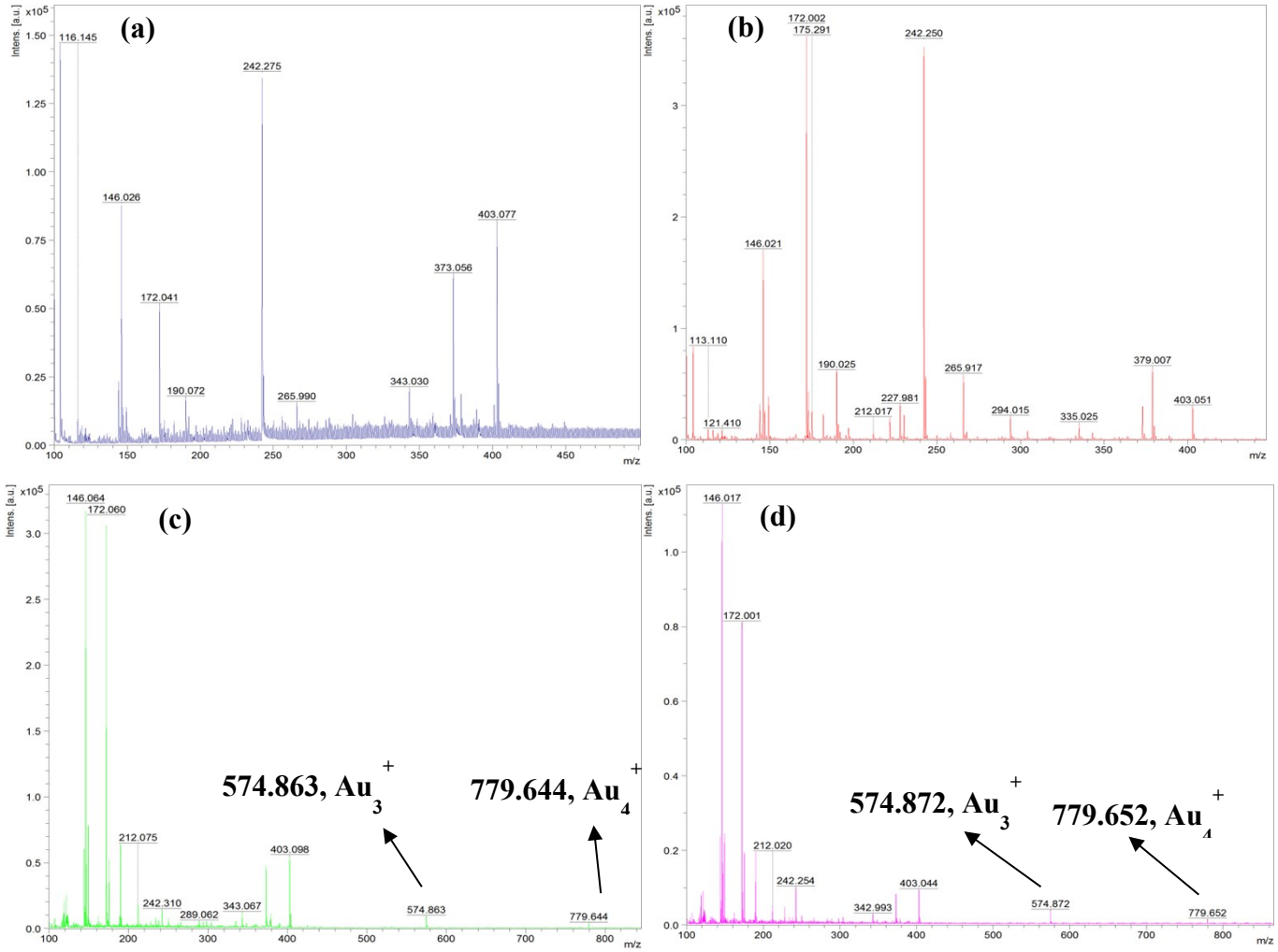

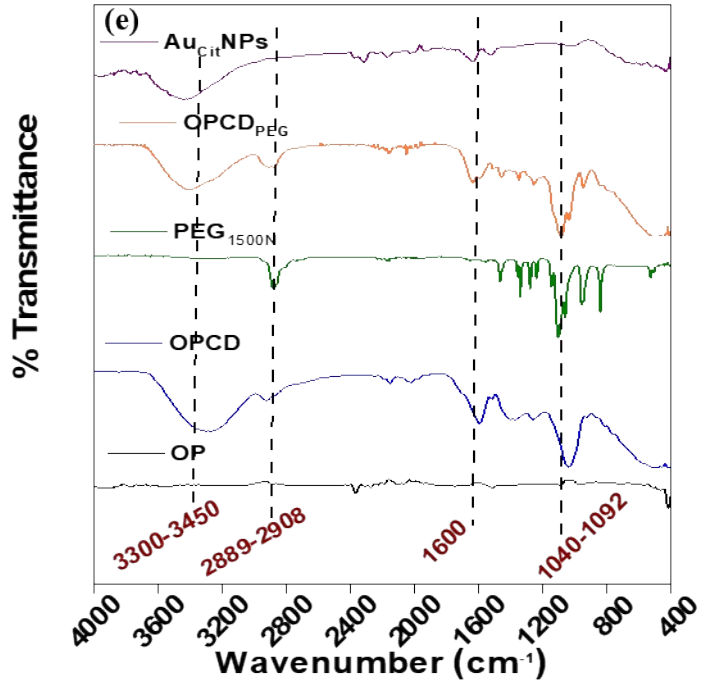

Figure S05. MALDI spectra of synthesized NPs viz., (a) OPCD, (b) $OPCD_{PEG}$, (c) $Au_{Cit}NPs$ and (d) $Au@OPCD_{PEG}$. (e) FTIR spectra of base material orange peel powder (OP), PEG_{1500N} along with OPCD, $OPCD_{PEG}$ and $Au_{Cit}NPs$.

Figure S06. Fluorescence and UV-spectroscopy studies

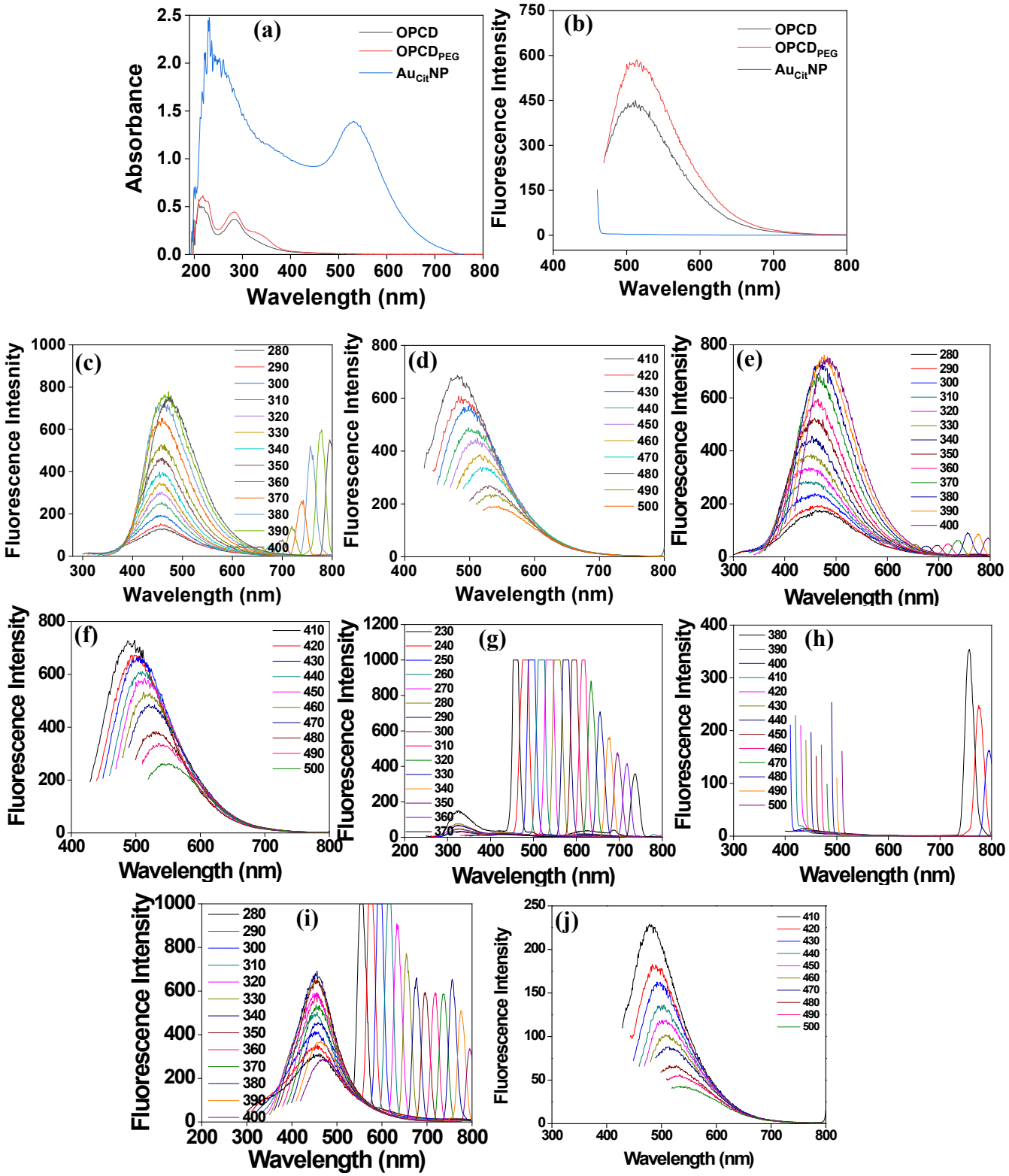

Figure S06. (a) Absorption and (b) selected fluorescence emission spectra of prepared NPs at

excitation of 450 nm. Fluorescence emission profile of synthesized NPs viz., (c, d) OPCD, (e, f) $OPCD_{PEG}$, (g, h) $Au_{Cit}NPs$ and (i, j) $Au@OPCD_{PEG}$.

Table S2 Quantum yield (QY) calculations

Sample	**Solvent**	**Refractive index**	**Ex/Em wavelength (nm)**	**Mean QY (%)**
Rhodamine 101	Ethanol	1.32	450/595	100
OPCD	Water	1.33	450/515	35.2±1.8
$OPCD_{PEG}$	Water	1.33	450/512	50.2±3.2
$Au@OPCD_{PEG}$	Water	1.33	450/505	14.2±2.3

Figure S07. Stability Studies

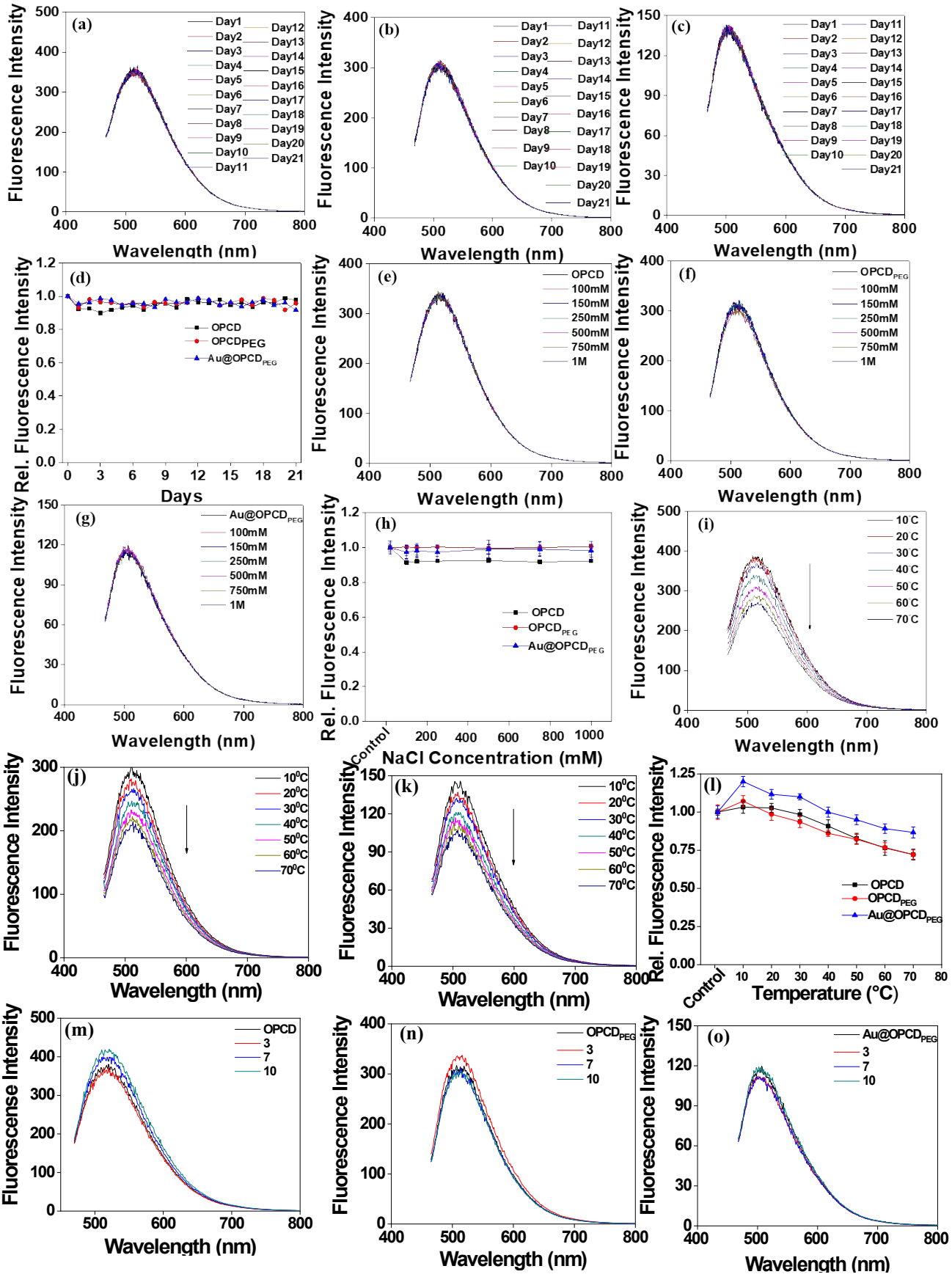

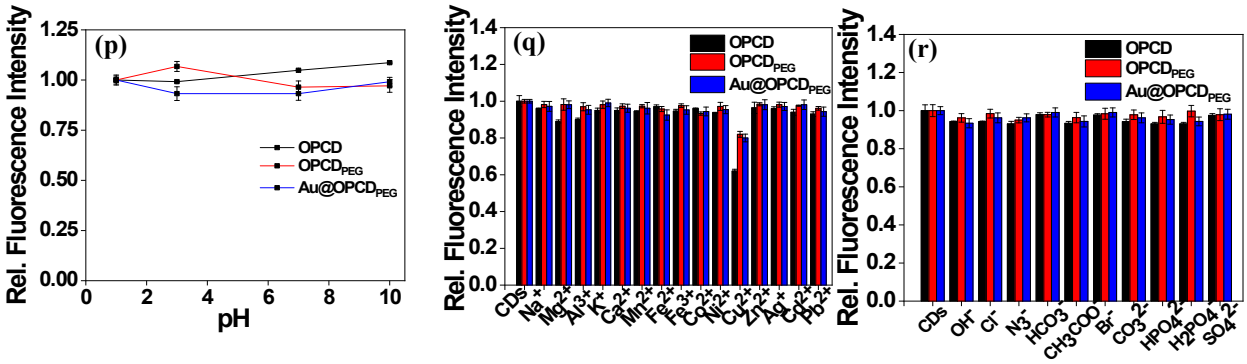

Figure S07. Fluorescence intensity changes of (a, e, i and m) OPCD, (b, f, j and n) $OPCD_{PEG}$ and (c, g, k and o) $Au@OPCD_{PEG}$ at different time interval, NaCl concentrations, temperature and pH variation. Corresponding relative intensity plots for all are given in d, h, l and p. Effect of (q) various metal cations and (r) anions on the fluorescence intensity of the synthesized NPs.

Figure S08. Fluorescence emission change of different NPs in presence of PYO and PyoV

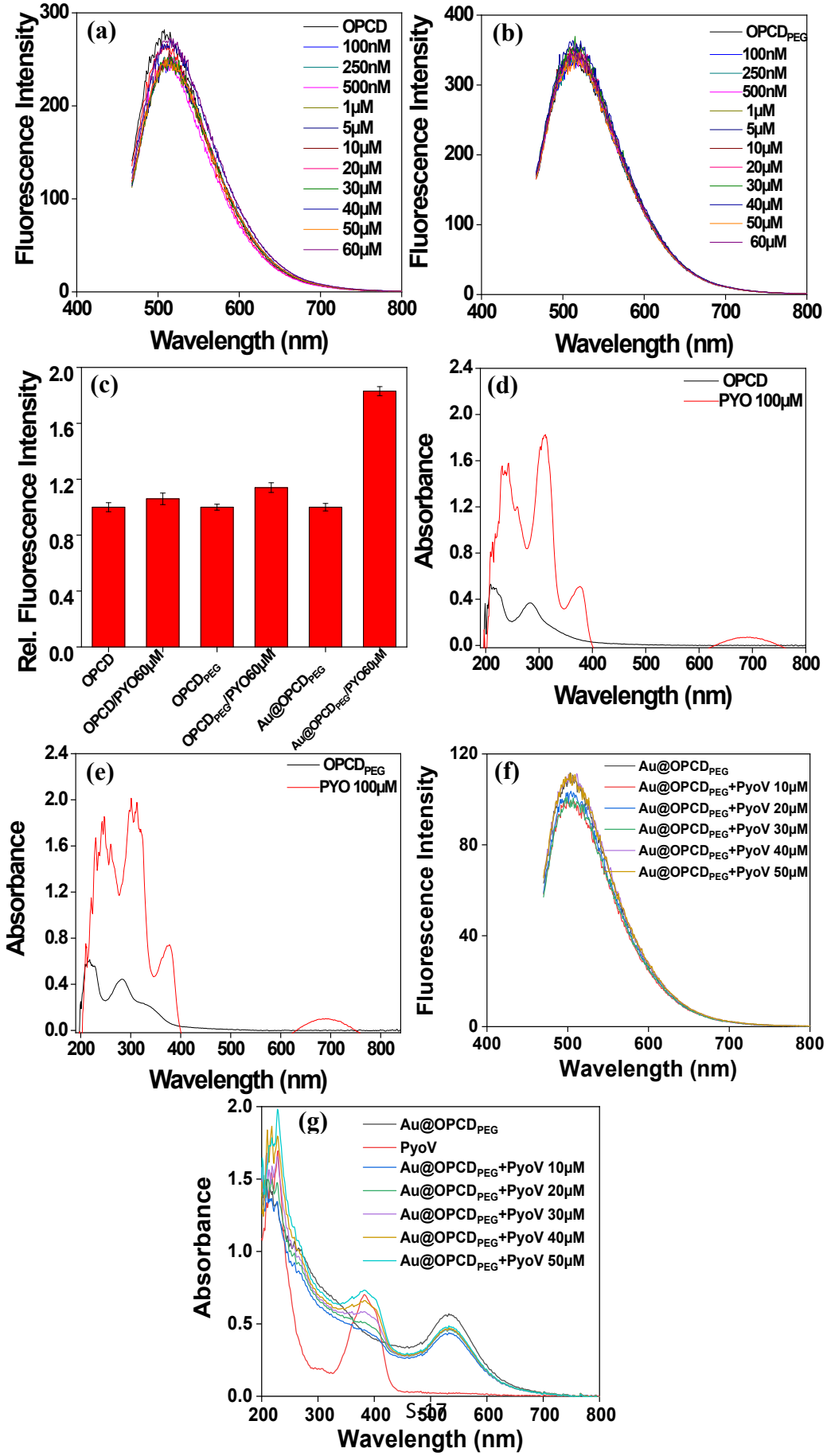

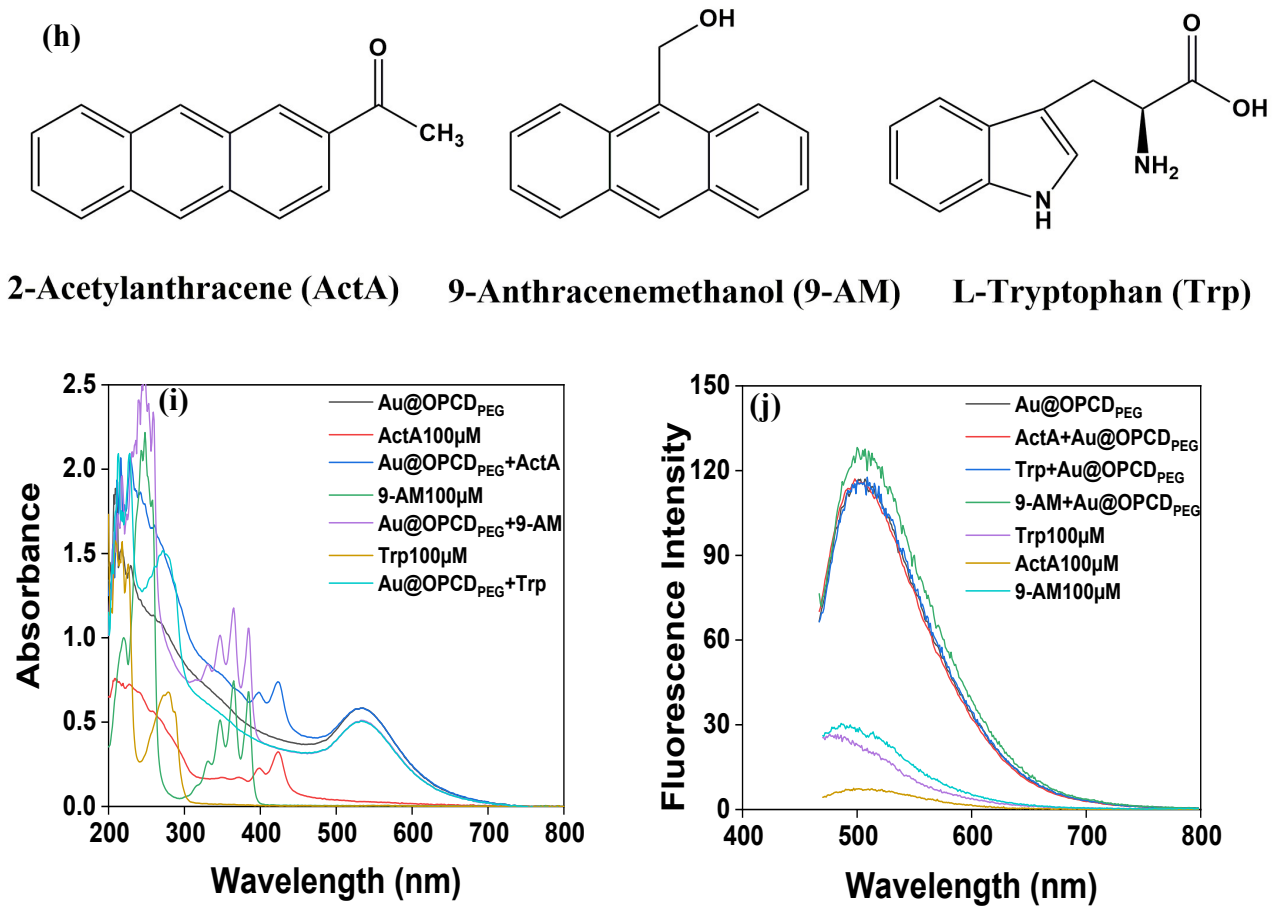

Figure S08. (a,b) Fluorescence emission profile of OPCD, $OPCD_{PEG}$ when interacted with varying concentration of PYO (100 nM to 60 µM). (c) The corresponding bar graph shows relative change in fluorescence intensity. (d) UV-Vis absorption profile of OPCD, (e) $OPCD_{PEG}$ when interacted with 100 µM of PYO. (f) Fluorescence and (g) absorption spectroscopy studies of $Au@OPCD_{PEG}$ when titrated with 10 to 50 µM of PyoV. (h) Chemical structure of different analyte used for the comparative studies, (i) absorption spectroscopy and (j) fluorescence spectra of titration of different analytes (100 µM) with $Au@OPCD_{PEG}$.

Figure S09. Limit of detection (LOD) studies

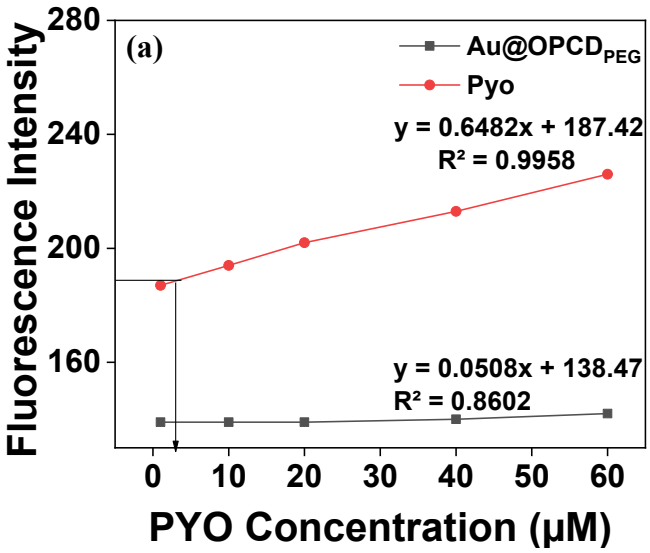

(b) Linear regression method for calculation of limit of detection and limit of quantification

Regression Statistics	
Multiple R	0.998716088
R Square	0.997433824
Adjusted R Square	0.996578432
Standard Error	0.888649499
Observations	5

ANOVA					
	Df	*SS*	*MS*	*F*	*Significance F*
Regression	1	920.8309062	920.8309062	1166.055	5.52145E-05
Residual	3	2.369093794	0.789697931	-	-
Total	4	923.2	-	-	-

	Coefficients	*Standard Error*	*t Stat*	*P-value*	*Lower 95%*	*Upper 95%*	*Lower 95.0%*	*Upper 95.0%*
Intercept	187.908586	0.629974415	298.2797105	8.31E-08	185.9037263	189.9134458	185.9037263	189.913446
X Variable	0.637076869	0.018656595	34.14754165	5.52E-05	0.577703256	0.696450482	0.577703256	0.69645048

Residual Output		
Observation	*Predicted Y*	*Residuals*
1	188.5456629	-0.545662906
2	194.2793547	-0.279354725
3	200.6501234	1.349876587
4	213.3916608	-0.39166079
5	226.1331982	-0.133198166

LOD= 3.3*Standard deviation of intercept/slope =3.3*0.62/0.63=3.26 µM

LOQ=10* Standard deviation of intercept/slope =10*0.62/0.63=9.88 µM

Figure S09. (a) Fluorescence based limit of detection studies after adding different concentrations of PYO *viz.,* 1, 10, 20, 40, 60 µM in the Au@OPCD$_{PEG}$ and (b) linear regression method for calculation of limit of detection and limit of quantification.

Figure S10. Relative fluorescence based PYO detection studies in competitive environment

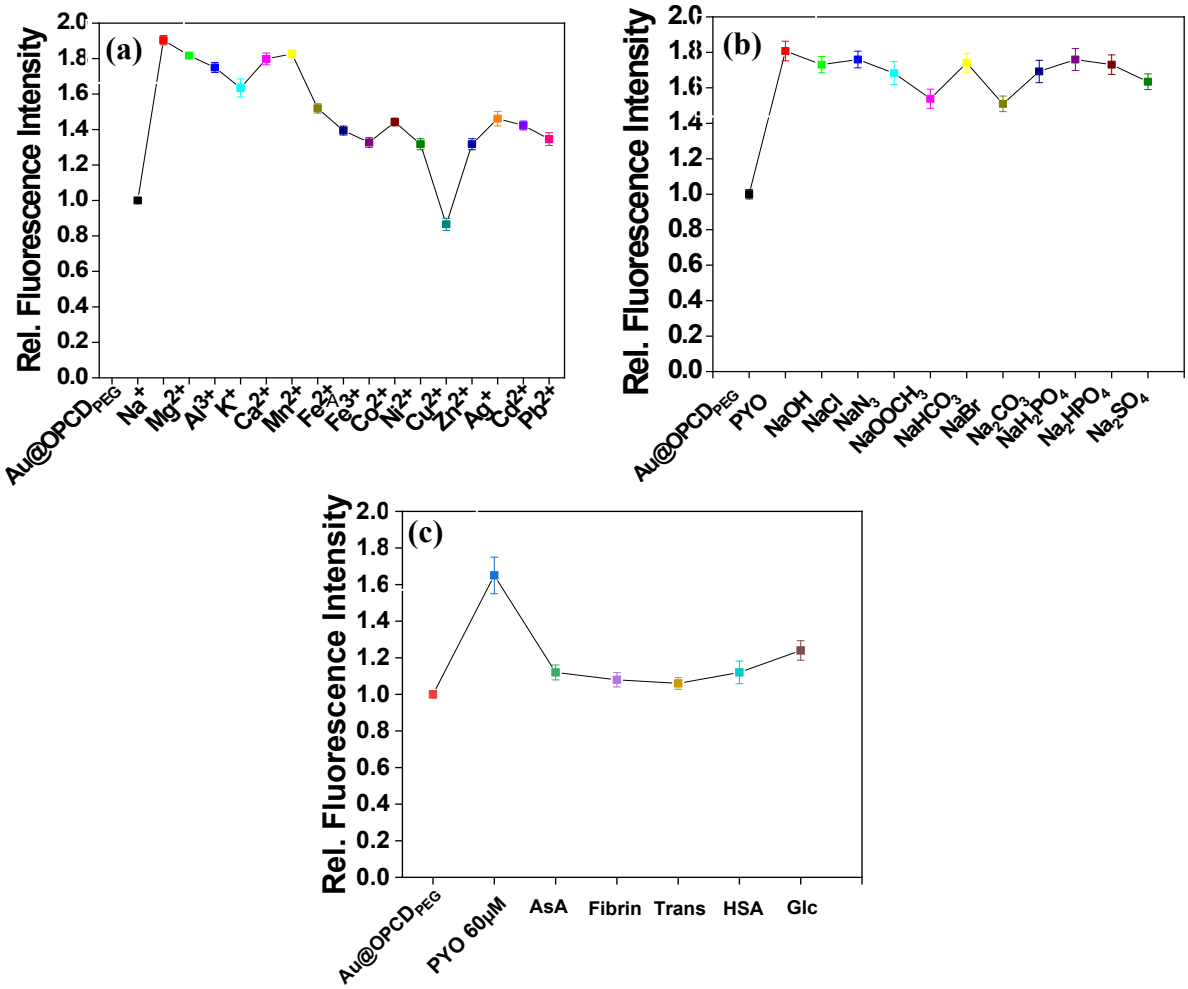

Figure S10. (a) Relative fluorescence-based detection studies of PYO in presence of competitive cations, (b) anions and (c) biomolecules.

Table S3. Percentage residual recovery studies of PYO in normal condition as well as when incubated in presence of human serum.

Added PYO (μM)	Detected (Normal)	% Recovery Rate (Normal)	Detected (Human sera)	% Recovery Rate (Normal)
15	14.8±0.03	98.6	13.3±0.12	88.6
25	24.9±0.81	99.6	26.6±0.04	106.1
45	46.1±0.36	102.4	47.3±0.12	105.12

Figure S11. bPYO extraction

(a)

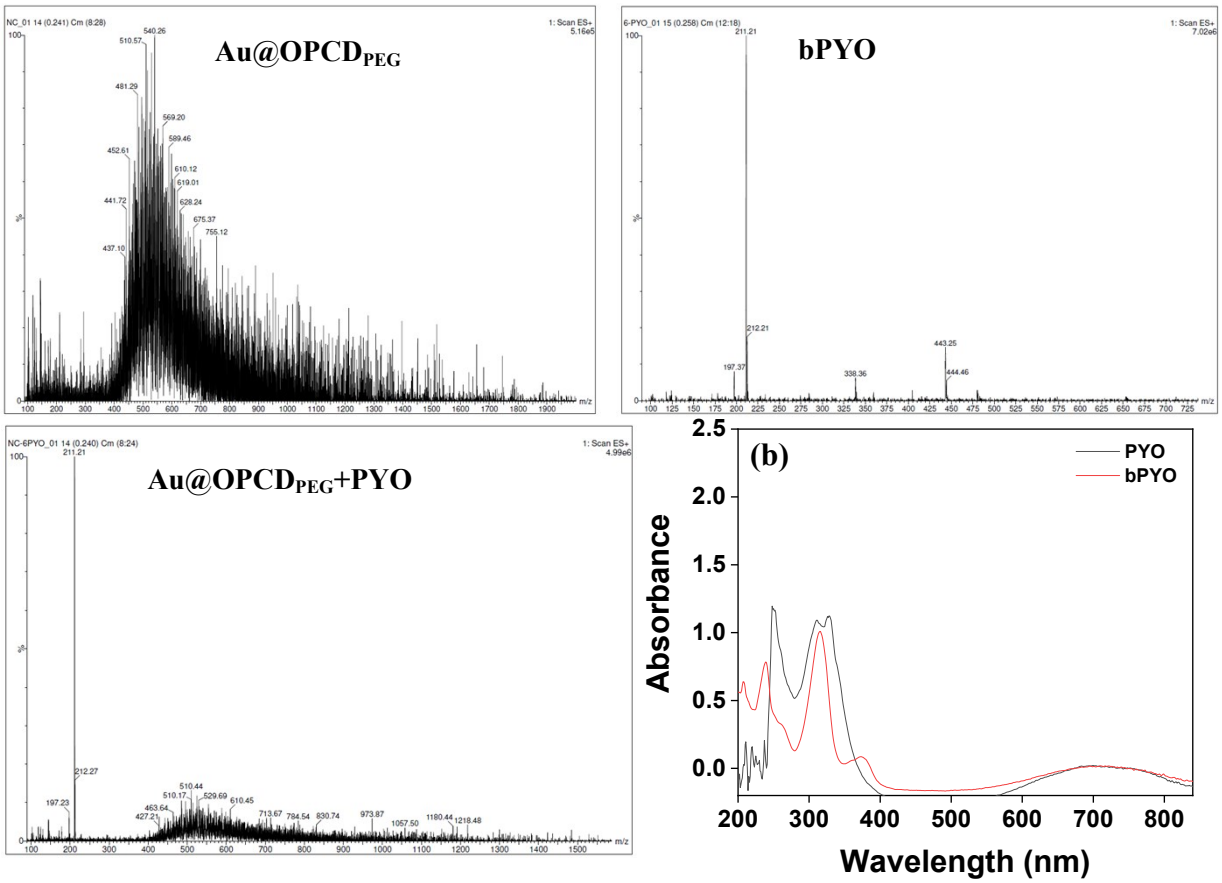

(c) Amount of bPYO extracted and detected in *P. aeruginosa* sample

18 ml of culture of P. aeruginosa = 0.75 X 1.5 X 10^8 X 18

= 202 X10^7 cfu ≅ 2.02 X 10^9 cfu

OD of extracted PYO at 520 nm = 0.22

Concentration of extracted PYO = OD X Extinction coefficient of PYO at 520 nm

= 0.22 X 17.1

= 3.76 µg/ml

1 ml of culture produces = 1.12 X 10^8 CFU ≅ 3.76 µg/ml PYO

LOD = 3.04 µM ≅ 639.1 µg of PYO

3.76 µg of PYO produced by =1.12 X 10^8, 639.1 µg of PYO produced by = 1.9 X 10^6 cfu

LOD=3.04µM=10^6 cfu

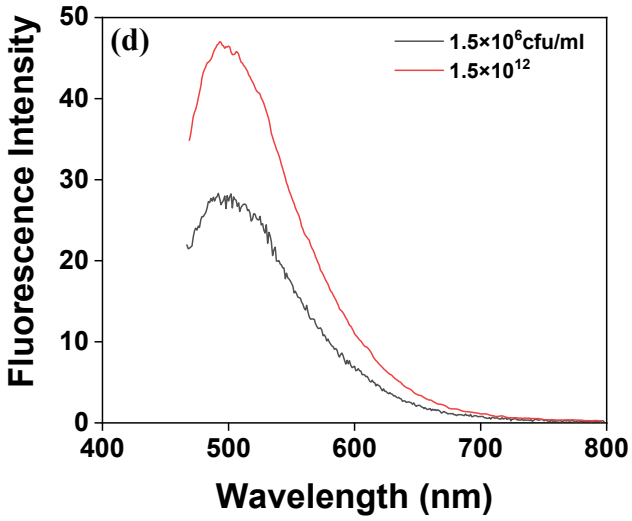

Figure S11. (a) ESI-MS of Au@OPCD$_{PEG,}$ bPYO and Au@OPCD$_{PEG}$ treated with PYO (b) Comparative UV-Vis absorption spectra of PYO and bPYO and (c) calculation for amount of bPYO extracted and detected in *P. aeruginosa* sample (d) Fluorescence intensity plot of different concentration of *P. aeruginosa* (cfu/ml).

Figure S12. Anti-bacterial activity

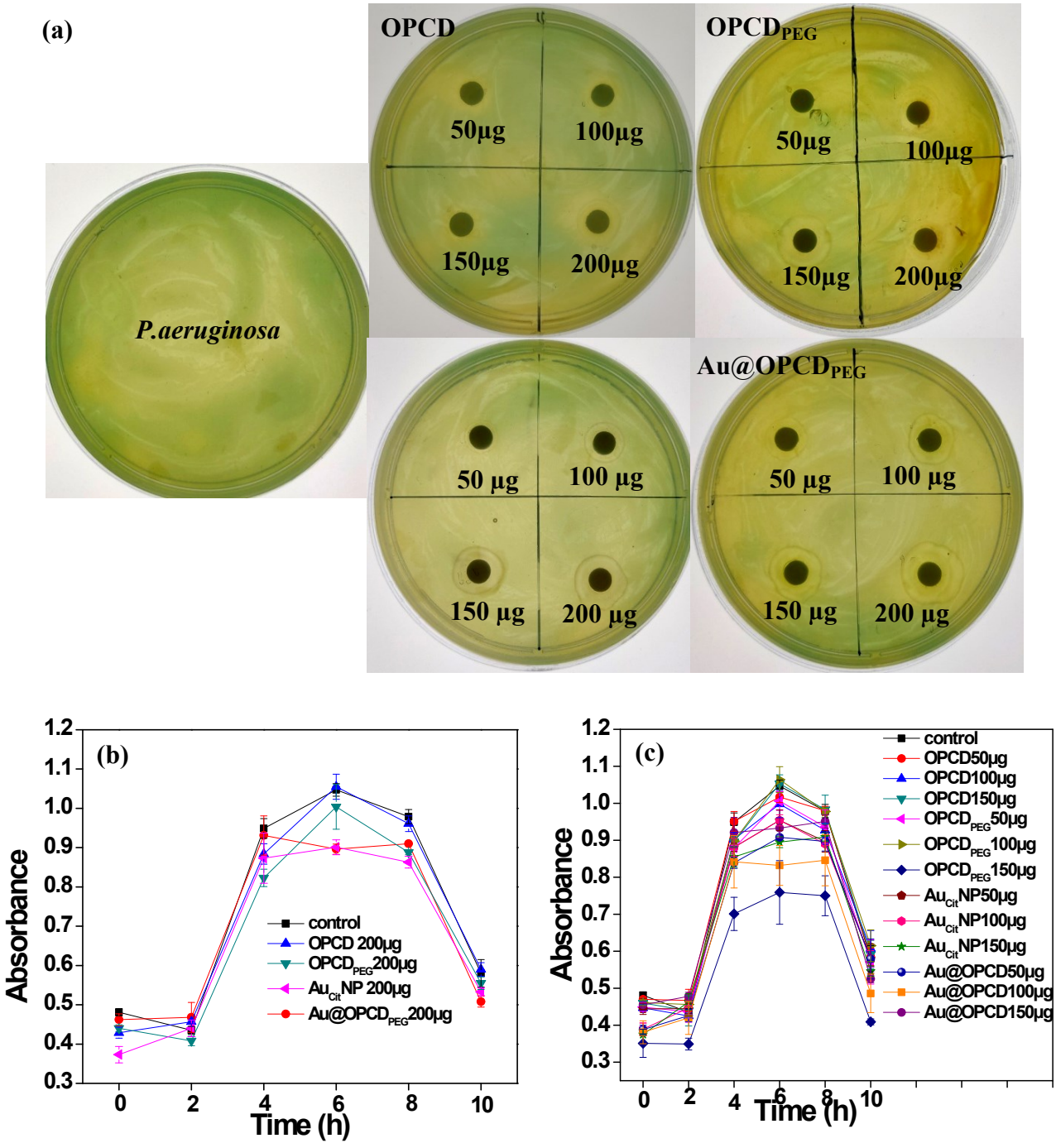

Figure S12. Anti-bacterial efficacy evaluation of the synthesized NPs. (a) Photographic images of the zone of inhibition (ZOI) developed during disc diffusion method for different control molecules and NPs. The studies were performed at different concentrations ranging

from 50 – 200 µg/ml. (b, c) Represents the growth inhibition curve for all the samples over a period of 10 h.

Table S4. Phase wise growth inhibition of *P. aeruginosa* at 200 µg/ml concentrations of prepared NPs; [not detected (ND)]

Growth Phase	**Nanomaterials**	**% Inhibition**
Lag Phase	OPCD	ND
	$OPCD_{PEG}$	6.9
	$Au_{cit}NP$	4.87
	$Au@OPCD_{PEG}$	ND
Log Phase	OPCD	ND
	$OPCD_{PEG}$	3.84
	$Au_{cit}NP$	13.4
	$Au@OPCD_{PEG}$	13.5
Stationary Phase	OPCD	1
	$OPCD_{PEG}$	9.27
	$Au_{cit}NP$	11.3
	$Au@OPCD_{PEG}$	6.18
Decline Phase	OPCD	1.6
	$OPCD_{PEG}$	6.77
	$Au_{cit}NP$	10.1
	$Au@OPCD_{PEG}$	15.25

Figure S13. Residual biofilm mass assay

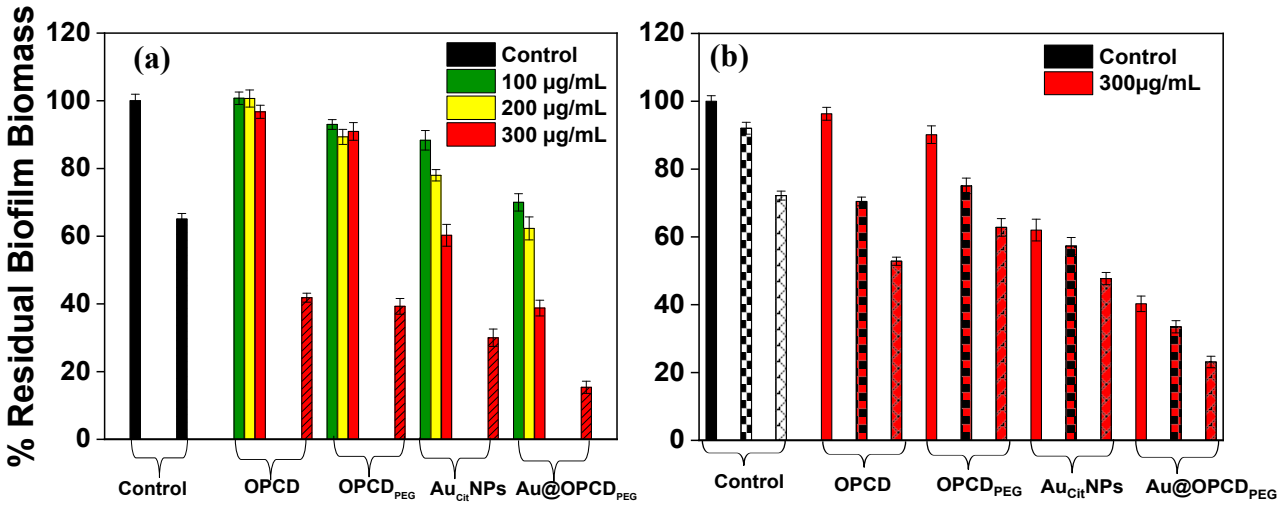

Figure S13. (a) Percentage of residual biofilm mass through crystal violet assay. The studies were performed at different concentrations ranging from 100 – 300 µg/mL. The laser irradiation studies were done with 300 µg/mL concentration of NPs (irradiated at 530 nm for 15 min). shaded bars (▮) are for photoirradiation studies for 15 mins for respective NPs)

(b) Antibiofilm activity of NPs (300 µg/mL) under laser irradiation condition at 5 (▮) and 10 (▮) min, respectively.

Table S5. Comparative calculations for crystal violet assay for residual biofilm mass after 12 h under normal condition and under photothermal treatment after laser irradiation at 530 nm for 15 min.

NPs	After 12 h (300 µg/ml)	After 15 mins (300 µg/ml) (530nm)
OPCD	96	42
$OPCD_{PEG}$	94	40
$Au_{Cit}NPs$	60	30
$Au@OPCD_{PEG}$	39	15

Figure S14. Cell viability assay

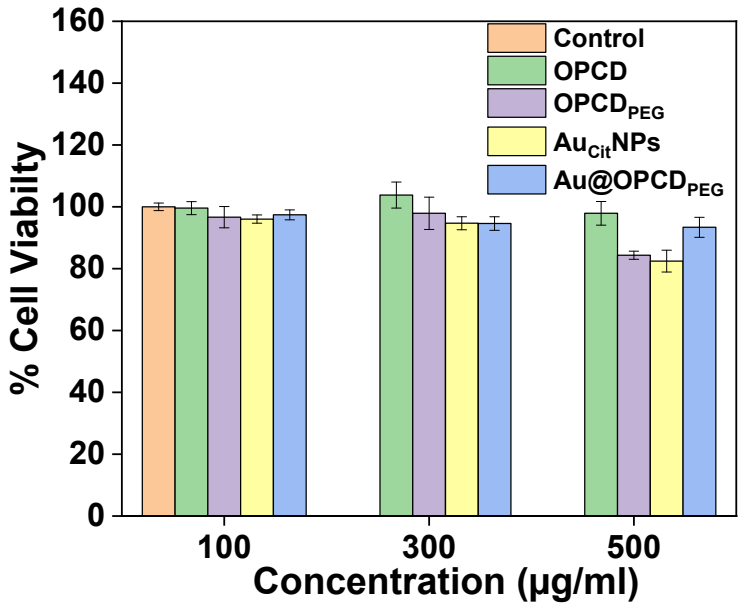

Figure S14. MTT assay to check cell viability of HEK 293 cells after 24 h

Figure S15. Antibiofilm activity

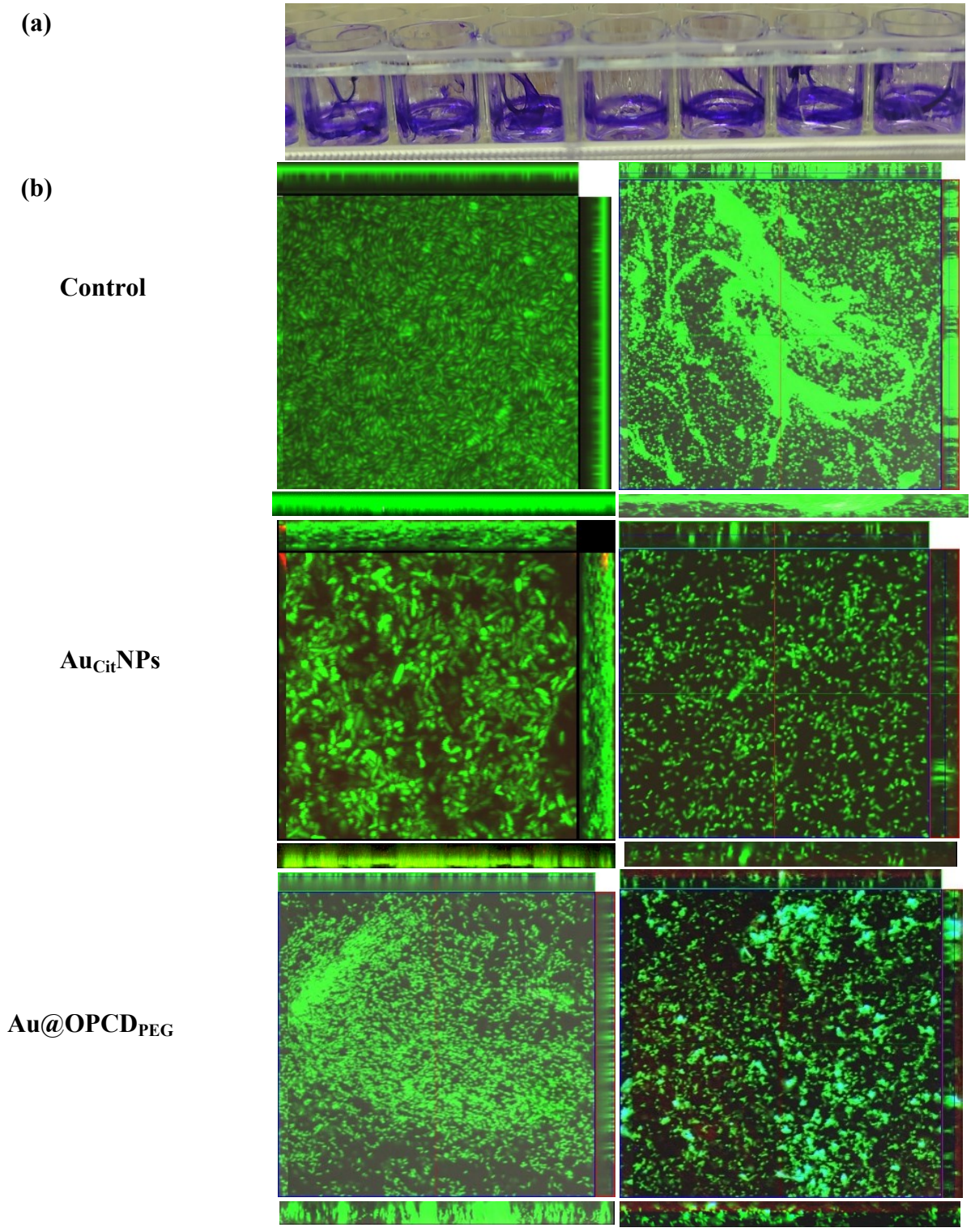

Figure S15. (a) Photographic images of crystal violet staining of biofilm. (b) Z-stack images of *P. aeruginosa* under normal (left) and photothermal irradiation condition (right) at 530 nm for 15 min.

Figure S16. Zeta potential and particle size to evaluate antibiofilm activity

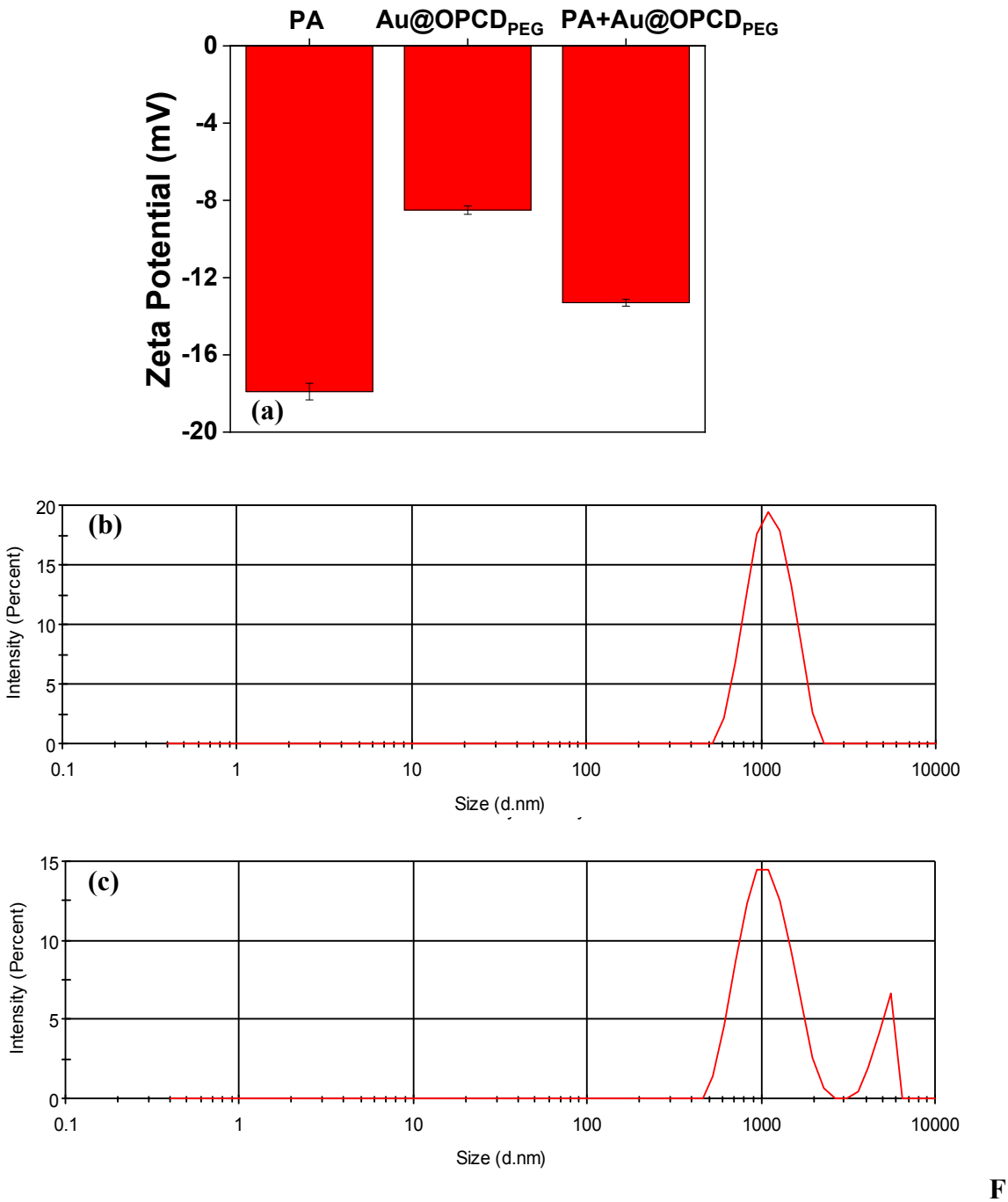

Figure S16. (a) Zeta potential and (b) and (c) hydrodynamic particle size of *P. aeruginosa* (PA) and Au@OPCD$_{PEG}$ incubated with PA, respectively.

Figure S17. Particle size and UV-Vis spectroscopy

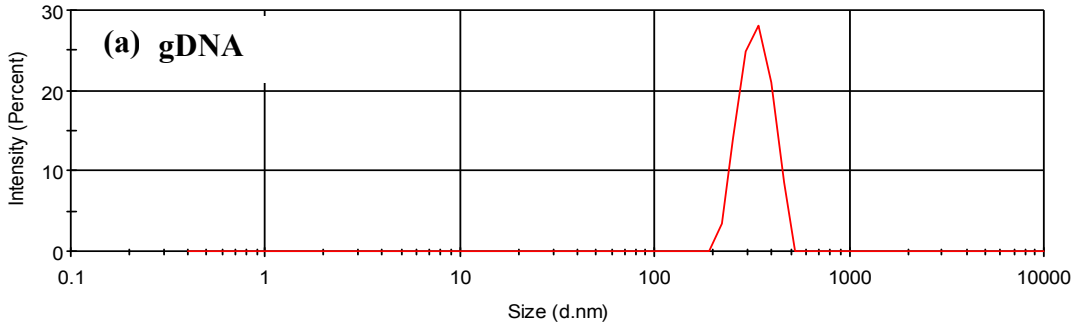
(a) gDNA
Intensity (Percent)
Size (d.nm)

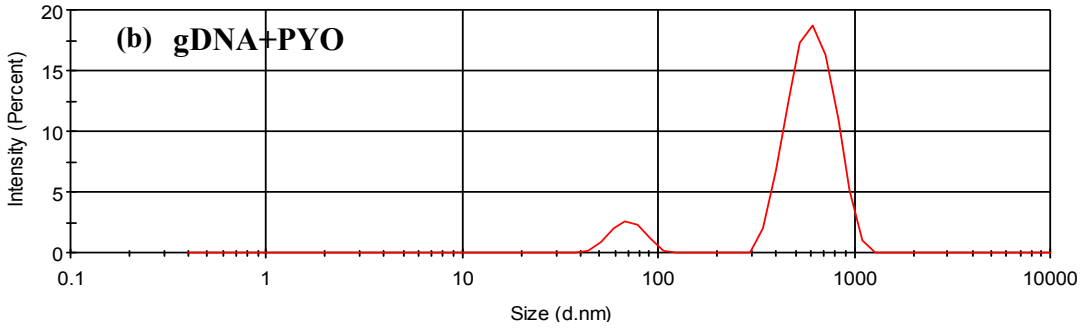
(b) gDNA+PYO
Intensity (Percent)
Size (d.nm)

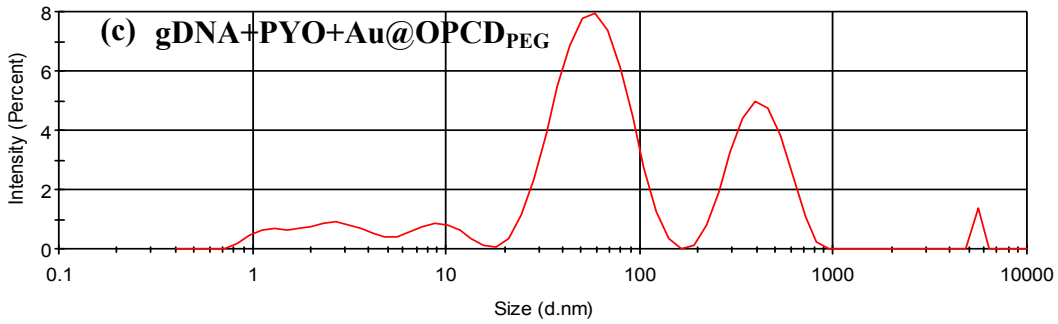
(c) gDNA+PYO+Au@OPCDPEG
Intensity (Percent)
Size (d.nm)

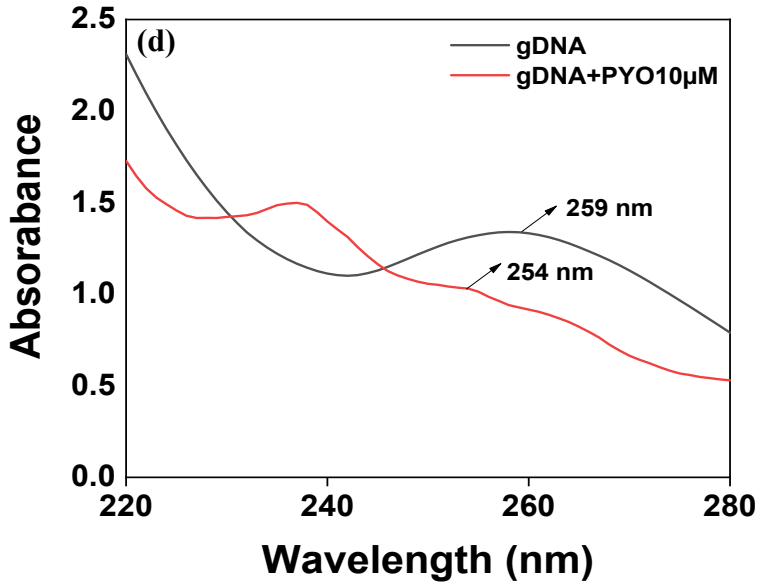
(d)
gDNA
gDNA+PYO10μM
259 nm
254 nm
Absorabance
Wavelength (nm)

Figure S17. (a-c) Hydrodynamic particle size of gDNA, gDNA and PYO mixture and Au@OPCD$_{PEG}$ NPs in presence of gDNA and PYO mixture, respectively. (d) UV-Vis spectra of gDNA and gDNA in presence of PYO (10µM).

Table S6. Hydrodynamic particle size of gDNA, complex of gDNA with PYO and gDNA, Au@OPCD$_{PEG}$ PYO (10µM)

Sample	**Z-average (nm)**	**Peaks**	**Percentage**
gDNA	637.6	335.4±62.1	100
gDNA + PYO 10µM	681.1	622.3±161	90.8
		70.2	9.2
gDNA + Au@OPCD$_{PEG}$ + PYO 10µM	147.6	59.8	57.5
		424.6	27.5